

Switching dynamics between the metastable ordered magnetic state and a nonmagnetic ground state: A possible mechanism for photoinduced ferromagnetism

Masamichi Nishino and Kizashi Yamaguchi

Department of Chemistry, Graduate School of Science, Osaka University, Toyonaka, Osaka 560, Japan

Seiji Miyashita

Department of Earth and Space Science, Graduate School of Science, Osaka University, Toyonaka, Osaka 560, Japan

(Received 6 May 1998; revised manuscript received 1 July 1998)

By studying the dynamics of the metastable magnetization of a statistical mechanical model we propose a switching mechanism for photoinduced magnetization. The equilibrium and nonequilibrium properties of the Blume-Capel model, which is a typical model exhibiting metastability, are studied by mean-field theory and Monte Carlo simulation. We demonstrate reversible changes of magnetization with a sequence of changes of system parameters, which models the reversible photoinduced magnetization. The implications of our results for recent experiments on Prussian blue analogs are discussed. [S0163-1829(98)03138-5]

I. INTRODUCTION

During the past decade reversible changes of magnetization by magnetic field, electric field, and other external fields have attracted much attention not only because of academic interest but also because of the possibility for applications in devices.¹⁻⁴ Very recently Sato, *et al.* have found that magnetic properties of the Prussian blue analogs $K_{0.2}Co_{1.4}[Fe(CN)_6] \cdot 6.9H_2O$ (Ref. 3) and $K_{0.4}Co_{1.3}[Fe(CN)_6] \cdot 5H_2O$ (Ref. 4) can be switched from the paramagnetic to the ferrimagnetic state (or vice versa) by visible and near-IR light illumination.

According to the experiments,^{3,4} Fe(II)-CN-Co(III) moieties in these compounds are responsible for the photoinduced effect. In the ground state Fe and Co are in a closed-shell structure which is nonmagnetic. However, when illuminated at a wavelength $\lambda_1 = 500-700$ nm, the oxidation states of Fe and Co change from Fe (t_{2g}^6 , $S=0$) and Co (t_{2g}^6 , $S=0$) to Fe (t_{2g}^5 , $S=1/2$) and Co ($t_{2g}^5 e_g^2$, $S=3/2$), respectively. These magnetic moments couple antiferromagnetically, resulting in a ferrimagnetic magnetization at low temperatures. The order persists after the illumination is stopped. Thus, the paramagnetic material is converted to a ferrimagnetic one by illumination and three-dimensional long-range magnetic ordering appears. After illumination at a different wavelength $\lambda_2 = 1319$ nm, the ferrimagnetic ordered state is switched back to the original nonmagnetic state. The switching can be reproduced very reliably. In short, these materials show two stable macroscopic states at low temperatures: a paramagnetic state and a ferrimagnetic ordered state and these bistable states can be switched reliably by using illumination.

We think that the competition between the following two factors is one of the keys to understanding this "switching" phenomenon: There is an energy cost associated with the creation of the magnetic moments at each site. But this cost can be compensated by the exchange coupling between the magnetic moments which promotes long-range order.

This sort of macroscopic switching phenomenon is an in-

teresting problem in the context of the dynamics of ordered states. Thus in this paper we propose a statistical mechanical mechanism for such switching based on a simplified model. In the equilibrium state, the physical properties must be unique functions of the system parameters. However, if the system has metastable states beside the equilibrium state, the system will exhibit hysteresis. This is the key mechanism underlying the switching effect.

The metastability is associated with a first-order phase transition. Thus in order to investigate the switching phenomena, we consider a model with the following properties: The ground state is nonmagnetic and the true thermodynamic state is paramagnetic, but the system has a very long-lived metastable ferromagnetic excited state. To this end, we adopt the Blume-Capel (BC) model, which is a ferromagnetic $S=1$ Ising model ($S^z = \pm 1$ or 0) with a crystal-field splitting for easy-planar symmetry:

$$\mathcal{H} = -J \sum_{\langle i,j \rangle} S_i S_j + D \sum_i S_i^2, \quad (1)$$

where J is the exchange constant and D is the crystal-field splitting and $\langle i,j \rangle$ indicates that the summation is over all nearest-neighbor pairs on a lattice. We study the model on the simple cubic lattice with the linear dimension L . This D expresses the excitation energy from a nonmagnetic state to a magnetic state. The spin S_i at a site represents a local magnetic state ($S_i = \pm 1$) or nonmagnetic state ($S_i = 0$). We deal with ferromagnetic interaction ($J > 0$) and positive D . The BC model was originally proposed as a way to study first-order magnetic phase transitions.^{5,6}

In this BC model the ordered state is ferromagnetic. On the other hand, for the materials used in the experiments the magnetic moments of different spins are coupled antiferromagnetically resulting in a ferrimagnetic order. However, the mechanism underlying the switching is the existence of a metastable ordered state due to the competition between the magnetic interaction (J) and local excitation energy (D). Thus, the BC model is a simple model which captures the

essential physics. More complicated models for individual systems could be provided if necessary.

In order to switch between the bistable states of the model, we make a sequence of changes of the effective parameters of the Hamiltonian due to the illumination. When photosensitive materials are illuminated, we generally expect that their physical properties change. The Kerr effect is a typical example, where the refractive index changes with the amplitude of the light. We expect that the parameters of the system, such as D and the temperature T , would be altered during the illumination, $(D, T) \rightarrow (D', T')$, returning to the original values when illumination ceases $(D', T') \rightarrow (D, T)$. During the illumination the state of the system evolves to the equilibrium state for (D', T') . However, after the illumination stops the system may not return to its original state because of the bistability. Thus such illumination would provide a switching procedure.

Using a Monte Carlo simulation, we demonstrate reversible switching of the magnetization with a sequence of changes of parameters (D, T) . We predict various features of the switching, such as, a relationship between the magnetization during the illumination and the state after the illumination. Depending on the effective parameters of the system during the illumination, the state after illumination is either magnetic or nonmagnetic. However, if the effective parameters take intermediate values, the state after the illumination becomes very stochastic. Namely, the switching may fail with some probability. This effect is also studied.

In Sec. II, we study the thermodynamic properties and the nature of the metastability of the BC model. In Sec. III, a mechanism for the reversible switching is proposed. Summary and discussion are given in Sec. IV.

II. THERMODYNAMIC PROPERTIES OF THE BC MODEL

A. Phase transitions and phase diagram

Thermodynamic properties of the BC model and extended BC models have been studied extensively, using mean-field approximation,⁵⁻⁷ renormalization,⁸⁻¹⁰ and Monte Carlo methods.^{11,12} In particular, the tricritical point between the second-order transition line and the first-order transition line has been investigated by various methods.¹³⁻¹⁶

In Fig. 1 we present the phase diagram in the (D, T) plane, where the points indicated by circles have been determined by Monte Carlo simulations. For small values of D the phase transition is second order. The critical temperatures are determined from the cross point in the Binder plot of the magnetization¹⁹ which are plotted by closed circles. On the other hand, when D is close to 3, this system has a first-order phase transition which is shown by the open circle.

Here we use the following simplified method to determine the first-order phase transition point, although there are several elaborate methods making use of the histogram of the order parameter.²⁰ We perform a simulation with a disordered initial state and decrease the temperature gradually, and find a temperature, (say, T_L), at which the system jumps to the ordered state. Then we perform another simulation with a complete ordered initial state at a low temperature and increase the temperature gradually to find a temperature (T_H)

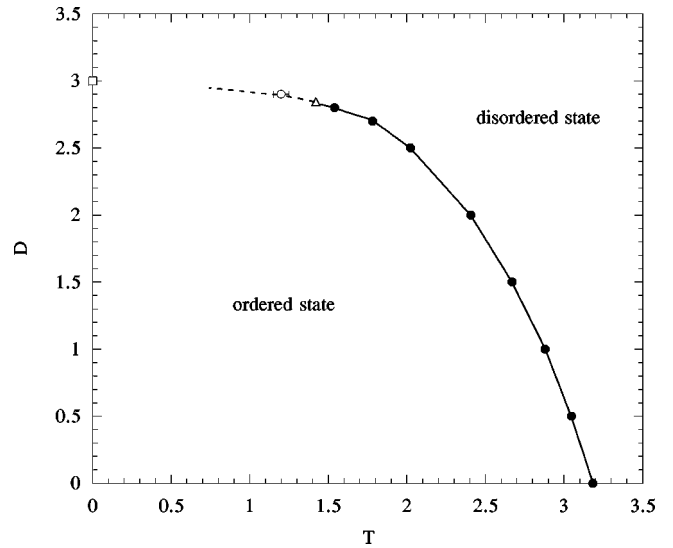


FIG. 1. The phase diagram of the BC model. The closed circles denote the second ordered phase transition obtained by a Monte Carlo simulation. The triangle denotes the tricritical point determined by Deserno. The open circle denotes the first-order phase transition obtained by a Monte Carlo simulation. The error bar denotes the region of the hysteresis.

at which the system jumps to the disordered phase. If T_L and T_H are separated significantly, then we regard the phase transition as first order.

In order to determine the critical temperature we performed the following simulations in $T_L < T < T_H$: we prepare an initial configuration in which half of the system is in the ordered state and the other half is in the disordered state. We then perform Monte Carlo simulations with different sequences of random numbers (in most cases we used 30 samples). If all the samples reach to the ordered phase, then we regard the set of the parameters (D, T) as belonging to the ordered state. On the other hand, if all the samples reach the disordered phase, then the set of parameters is regarded as belonging to the disordered state. If the samples distribute among both phases, we suppose that this (D, T) is in the critical region. The error bar in Fig. 1 shows the maximum range of this critical region and the open circle is put in the middle of this region.

This procedure was carried out for $L=10$. If we increase the size of the system the error bar would shrink. However for the purpose of the present paper, we need only a rough phase diagram and Fig. 1 is satisfactory. The triangle shows the position of the tricritical point obtained by Deserno,¹⁶ which locates consistently in Fig. 1. This in turn demonstrates the reliability of the present computations.

B. Metastability of the BC model

As has been mentioned in the Introduction, the BC model has metastable states.^{17,18} First we investigate the free energy as a function of the magnetization using a mean-field approximation:

$$F(M) = -k_B T \ln[\text{Tr} \exp(-\beta \mathcal{H}_{\text{MF}}(M))] + \frac{1}{2} \beta J z M^2 \quad (2)$$

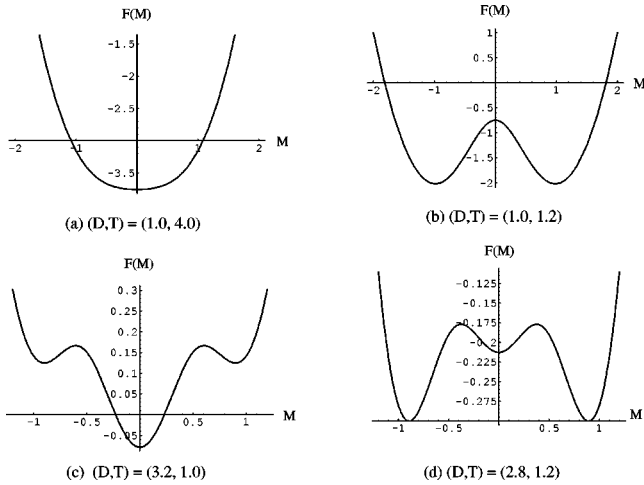


FIG. 2. The mean-field free energies of the BC model for various parameter sets (D, T) .

with

$$\mathcal{H}_{\text{MF}}(M) = zJMS - DS^2, \quad (3)$$

where β is $1/k_B T$, M is the mean magnetization per site and z is coordination number which is 6 for the simple cubic lattice. The free energy is explicitly given by

$$F(M) = -k_B T \ln[2 \exp(-\beta D) \cosh(\beta J z M) + 1] + \frac{1}{2} \beta J z M^2. \quad (4)$$

Hereafter we take J as a unit of energy and put $k_B = 1$.

At $T=0$ the system is nonmagnetic ($M=0$) for $D > 3.0$, while it is completely ferromagnetic ($M=1$) for $D < 3.0$. In Figs. 2, $F(M)$ for typical cases are illustrated: First let us consider the case of $D=1.0$ and $T=4.0$. In this case the system is paramagnetic and $F(M)$ has a single minimum

[Fig. 2(a)]. In the mean-field treatment, the tricritical point (D_t, T_t) is found to be $(2.7726, 2.0)$,⁷ which is plotted by a triangle in Fig. 3. If D is smaller than that of the tricritical point, the system shows a second-order phase transition and $F(M)$ has a double minima [Fig. 2(b) for $D=1.0$ and $T=1.2$]. Furthermore $F(M)$ can have three minima due to the existence of the metastable state. In the case where the nonmagnetic state is the true equilibrium state the system has a metastable ferromagnetic state [Fig. 2(c) for $D=3.2$ and $T=1.0$]. The metastable nonmagnetic state is also possible at $D < 3$ where the ferromagnetic state is the true equilibrium state [Fig. 2(d) for $D=2.8$ and $T=1.2$]. These four types of structure characterize the nature of the states of the BC model.

In Fig. 3, we show a phase diagram including the metastable region in the mean-field free energy (4). First consider the case where D is smaller than D_t . When the temperature decreases, the shape of the free energy changes as [Fig. 2(a) (the paramagnetic region, hereafter we refer to this region as I) \rightarrow Fig. 2(b) (an ordered state, region II) \rightarrow Fig. 2(d) (an ordered state with a metastable paramagnetic state, region III)]. The boundary between I and II is the second-order equilibrium phase transition line and is shown by a solid line. On the other hand, the boundary between II and III (dash-dotted line) does not correspond to any equilibrium phase transition but it shows a boundary where metastability appears. On these lines the coefficient of M^2 of $F(M)$ vanishes. These lines join at the point labeled Q, $(D_Q, T_Q) = (2.7783, 1.899)$. The value of D at this point is larger than D_t .

Next we consider the case where $3 > D > D_Q$. Here the shape of the free energy changes as [Fig. 2(a)–Fig. 2(c) (a paramagnetic state with a metastable ferromagnetic state, region IV) \rightarrow Fig. 2(d)]. At the boundary between I and IV, a metastable ferromagnetic state appears, which is shown by a dotted line. The boundary between III and IV (dashed line) is the first-order phase transition line in the equilibrium. In the

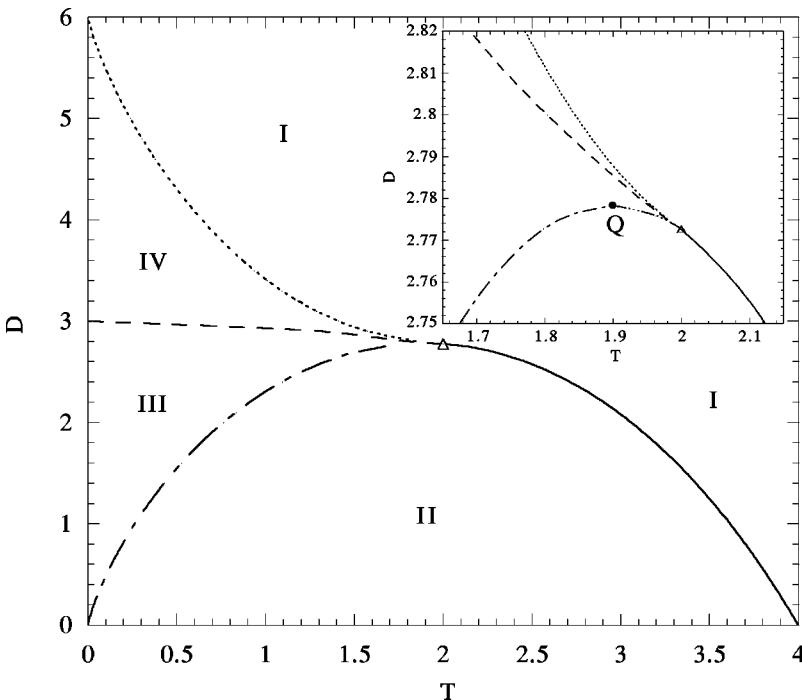


FIG. 3. The phase diagram including the metastable region in the mean-field theory (see text).

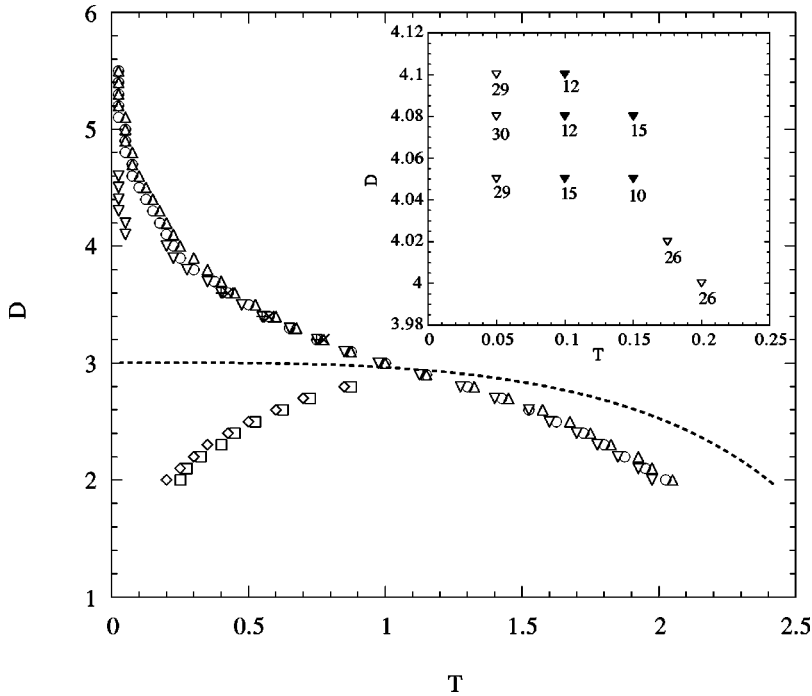


FIG. 4. The metastable ferromagnetic and paramagnetic region obtained by Monte Carlo method. The dashed line is the phase boundary shown in Fig. 1. The symbols denote the boundaries of the metastable region (for details, see text).

region between D_t and D_Q (see in the inset in Fig. 3), complicated changes of the shapes of $F(M)$ occur: [(a)→(c)→(d)→(b)→(d)].

For $D > 3$, thermodynamically the whole region is paramagnetic. However there exists a metastable ferromagnetic state IV. The boundary between I and IV is shown by a dotted line.

Next, we investigate the phase diagram for the metastability corresponding to Fig. 3 by a Monte Carlo simulation. In order to estimate the metastability, we adopt the following method: We performed simulations with a complete ferromagnetic initial configuration. If the ferromagnetic state is metastable, it would survive after long simulation. Thus we estimate its stability by counting the number of samples which remain in a ferromagnetic state after 10 000, 100 000 and 1 000 000 Monte Carlo Steps (MCS). Here we took the following criterion for the survival: If the magnetization of the system becomes smaller than 0.5 ($|\sum_i S_i| < 0.5L^3$), we regard that the state relaxes to the paramagnetic state. This value 0.5 is not very critical and could be 0.3, etc., because the metastable magnetization decays rather suddenly. These simulations were performed for $L = 10$ and 20 with periodic boundary condition.

In Fig. 4, we plot the highest temperature at which more than 2/3 of samples ($L = 10$ and 30 samples) remain in a ferromagnetic state after 10 000 MCS by upward triangles, after 100 000 MCS by circles and after 1 000 000 MCS by downward triangles. We find that boundaries of metastable regions with different MCS locate rather closely to one another. Therefore we conclude that the transition region between the simple paramagnetic region I and the metastable region IV is rather narrow and we can distinguish the boundary between I and IV rather clearly.

In the same way, we determine the metastable region for the disordered phase which is also shown in Fig. 4 ($D < 3$), by boxes (10 000 MCS) and diamonds (100 000 MCS). Qualitatively, the phase diagram in Fig. 4 agrees well with that of Fig. 3.

We have also studied the size dependence of the metastability of the ferromagnetic state. We expect that the metastable state in the present model is in the so-called stochastic region or single droplet region.²¹ There we expect the nucleation rate in the whole volume is about 8 times larger in the system of $L = 20$, because the volume of the system is eight times larger than that for $L = 10$. Actually in the cases with $D > 3.0$, we observe the boundary for 12 500 MCS (the symbol \times in Fig. 4) and 125 000 MCS (the symbol $+$ in Fig. 4) of the systems of $L = 20$ overlap well with those for 100 000 and 1 000 000 in the system of $L = 10$.

C. Detailed feature of the phase diagram



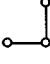
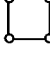
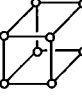
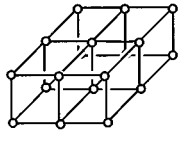
If we compare Fig. 4 with Fig. 3, although they agree with each other qualitatively, we find the following detailed features in Fig. 4. First, the transition is not sharp near $D = 4.0J$ for the data of 1 000 000 MCS. In the inset of Fig. 4, the number of samples which remain ferromagnetic are shown. Second, the boundary denoted by symbols (circles, upward triangles, and downward triangles) does not agree with the second-order phase-transition line in Fig. 1 (dotted line). The boundary shifts towards low temperature.

The physical mechanism of these features will be discussed below. In order to understand the broadening of the boundary, we investigate the boundary of the metastability of the complete ferromagnetic state from a view point of local nucleation process. Let us consider configurations with a cluster of nonmagnetic sites. The energy difference ΔE between the complete ferromagnetic state and a state with the cluster is given by

$$\Delta E = -nD + mJ, \quad (5)$$

where n is the number of nonmagnetic sites and m is the number of excited bonds (i.e., $S_i S_j = 0$). In Table I, the excess energies ΔE for various clusters of nonmagnetic sites are given. The complete ferromagnetic state is unstable even for a flip of a single site when $6J < D$. Thus the upper limit

TABLE I. Clusters of n nonmagnetic sites and the energy difference (ΔE) from the completely ferromagnetic state.

n	Configuration	ΔE
1		6J-D
2		11J-2D
3		16J-3D
4		20J-4D
	⋮	
8		36J-8D
	⋮	
18		75J-18D

of the metastability locates at $D=6J$. For $3J>D$, the ferromagnetic state becomes the true equilibrium state. Thus the metastable ferromagnetic state exists in the range $3J<D<6J$, which is consistent with the above analysis of the free energy. In this range, the excess energy of a cluster configuration, ΔE , increases as n increases for small values of n . Therefore the complete ferromagnetic state is stable against fluctuation with such small clusters. On the other hand, for large values of n , ΔE decreases when n increases. Between these two regions, ΔE has a maximum at $n=n_C$. The configuration for the maximum ΔE is called the critical nucleus. This means that once a cluster of nonmagnetic sites becomes larger than n_C , it grows to destroy the metastable ferromagnetic state. In Fig. 5, the minimum values of ΔE for a given n are plotted for various values of D .

The boundary of the metastability may be given by

$$e^{-\beta\Delta E(n_C)} \approx p_{\min}, \quad (6)$$

where p_{\min} is the smallest nucleation rate which is detectable in the observation (in Monte Carlo simulation in the present

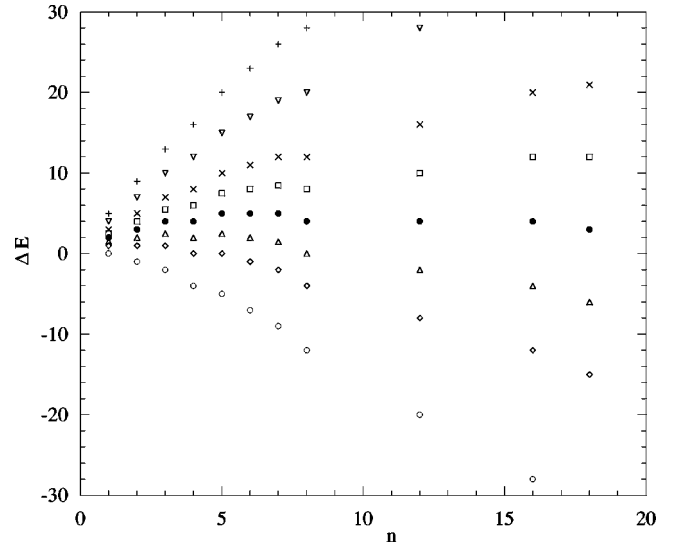


FIG. 5. Dependence of ΔE on the number of sites n for various values of D . Symbols +, ∇ , \times , \square , \bullet , \triangle , \diamond , and \circ denote data for $D=1, 2, 3, 3.5, 4, 4.5, 5$, and 6 , respectively. The maximum point corresponds to the size of the critical nucleus for each value of D .

case). Because we are studying phenomena in the time scale $t < 10^6$ MCS and the size of system $L^3 \approx 10^3$, we could detect in the simulation phenomena with probability $p \geq p_{\min} \approx 10^{-9}$. Because we are interested in the temperature region, $T < 0.5$, only the phenomena with ΔE of

$$\Delta E < 10J \quad (7)$$

are meaningful in the present observation because

$$e^{-\beta\Delta E} > p_{\min} \approx 10^{-9}. \quad (8)$$

For $D > 4J$, the ferromagnetic state is only stable against clusters with a few nonmagnetic sites. Thus the region of metastability exists only if $T \ll 1$. In the range ($\Delta E < 10J$) we find that $\Delta E(n)$ becomes very flat at $D=4$. Thus we expect that the boundary of the metastability becomes ill defined for this case, which would give the explanation of the wide range of the transition observed in Fig. 4.

Next, let us consider the shift of the boundary. This disagreement is simply due to the definition of the boundary introduced above, that is, the criterion that the system has decayed to the paramagnetic state if $M < 0.5$. For $D < D_t$, the ferromagnetic order is stable but not metastable. Thus here the position of the boundary does not mean the end of the metastability but the end of the ordered state. To detect the position of the boundary we use the threshold $M = 0.5$; this is appropriate because the metastable magnetization is close to 1.0 and decays suddenly. On the other hand, the fluctuation becomes large near the second-order phase transition and even in the ordered state (type II) M may easily become less than 0.5 as we discuss in the Appendix. For such a case the symbols (circles, etc.) locate on the lower temperature boundary of such a region where there are large fluctuation of the magnetization. Thus the region between the boundary shown in Fig. 4 (circles, etc.) and the second-order phase transition line (dashed line) is an ordered phase but with large fluctuation.

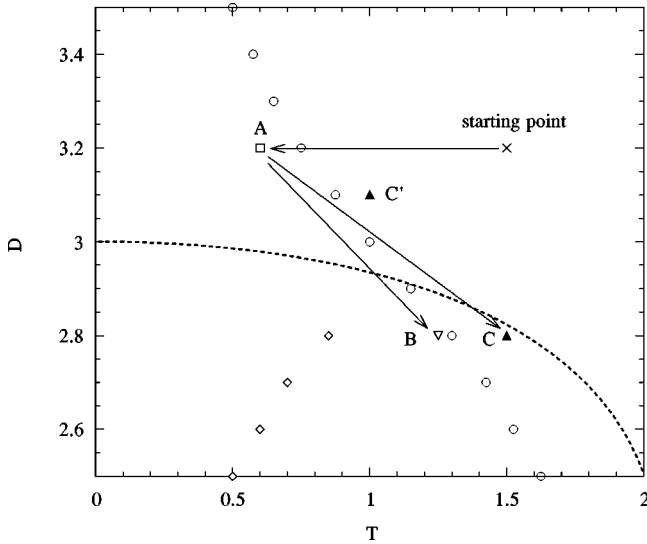


FIG. 6. Switching path in (D, T) plane with phase boundary and metastable regions. Definitions of A, B, C, and C' are given in the text.

III. REVERSIBLE SWITCHING

In this section we consider a possible mechanism of switching between the ordered state and disordered state, making use of the structure of metastability studied in the previous sections and demonstrate the mechanism by a Monte Carlo simulation. Here simulations are done in a system of $L=10$. We have checked that qualitative features do not change in the system of $L=20$ and even quantitatively most properties are reproduced in the system of $L=20$.

We consider a point (D, T) where the system is nonmagnetic in the equilibrium state but which has a long-lived metastable ordered state. We can find such a point in the present model with D a little bit larger than 3.0 at low temperature. We take a point A [$(D_A, T_A) = (3.2, 0.6)$] as such a point (see Fig. 6). Let the equilibrium paramagnetic state and the metastable ferromagnetic state be named α and α' , respectively.

If the system is put in other environments, such as under illumination, the parameters, J and D , would be renormalized. Let a point X (D_X, T_X) be such a state with renormalized parameters. Now we study the change of magnetization in the change of the parameters $A \rightarrow X \rightarrow A$. Here we take D_X to be 2.8 and study for various values of T_X .

First let us consider the case where T_X is in the ordered state, i.e., in region II but not in III. There the paramagnetic state is not metastable, and thus the system rapidly becomes ferromagnetic when the system moves to X. If T_X is low in this region, there exist only small clusters of nonmagnetic sites which are smaller than the critical nucleus for D_A . Thus state of the system will be trapped in the metastable ferromagnetic state when the system comes back from X to A. For such X we choose $T_X=1.25$. Hereafter we call this point B; $(D_B, T_B) = (2.8, 1.25)$ and call the state at B β . The change of magnetization for a change of parameter ($A \rightarrow B \rightarrow A \rightarrow B \dots$) is shown in Fig. 7.

To reach the state α , we start with a high temperature ($T=1.5$) and cool down the system. (If we start with complete ferromagnetic state at $T=0$ and warm up the system we find the state α' at A.) Practically, simulations were performed as follows: First we simulate the system at a high temperature $T=1.5$ with 50 000 MCS and then gradually reduce the temperature by $\Delta T=0.1$ iteratively until $T=0.6$. At each temperature 50 000 MCS are performed. This starting process will be also used in the following simulations. Next the system moved to the point B and 20 000 MCS is performed. Now the state is β . Then the system comes back to A and there another 100 000 MCS is performed, where we find that the state is the metastable ferromagnetic state (i.e., α'). In order to check the stability of the dynamics, we repeated this cycle.

Next, we take T_X at a higher temperature $T_X=1.5$, where many clusters of nonmagnetic sites are excited. This point will be called C; $(D_C, T_C) = (2.8, 1.5)$ and the state will be called γ . The change of magnetization is shown in Fig. 8, where the system at point A is always paramagnetic (α).

Whether the state after the system comes back from X is ferromagnetic or paramagnetic depends on the temperature T_X . For intermediate temperatures, the state after coming back from X distributes among ferromagnetic or paramagnetic state. For example the time evolution of the magnetization for $T_X=1.38$ is shown in Fig. 9. The state at this X is called δ . We investigate the reliability of the switching by making use of the quantity:

$$P = \left(\frac{N_f - N_p}{N_f + N_p} \right)^2, \tag{9}$$

where N_f is the number of appearance of ferromagnetic state and N_p is as well for paramagnetic state. This quantity indi-

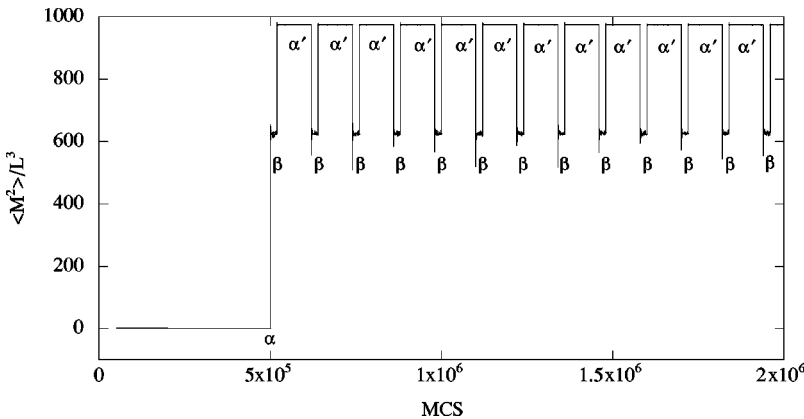


FIG. 7. The change for the square of magnetization per site $\langle M^2 \rangle / L^3$ in the case of $T_X=1.25$. α and α' denote the paramagnetic state and ferromagnetic state at A, respectively. β is a state at B.

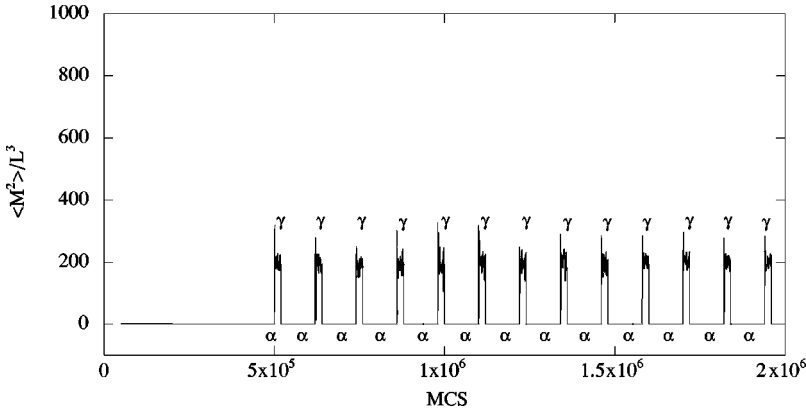


FIG. 8. The change for the square of magnetization per site $\langle M^2 \rangle / L^3$ in the case of $T_X = 1.5$. α denotes the paramagnetic state at A. γ is a state at C.

icates the degree of certainty of the state after the system comes back from X. If there exists a cluster of nonmagnetic sites which is larger than the critical size for D_A at X, the state will become nonmagnetic after coming back to A.

The distribution of the size of nonmagnetic cluster in X, $p_X(n)$, determines the distribution of N_f . The quantitative analysis for $p_X(n)$ is difficult but we expect that $N_p / (N_f + N_p)$ is a monotonic function of T_X and is very small for small T_X and $N_f / (N_f + N_p)$ is also very small for large T_X . Thus we can classify T_X into three regions: i.e., $N_p / (N_f + N_p) \approx 0$ ($P=1$), $0 < N_p / (N_f + N_p) < 1$ ($0 < P < 1$), and $N_p / (N_f + N_p) \approx 1$ ($P=1$) rather clearly.

In the simulation, we obtained P by counting N_f over 10 repetitions: $A \rightarrow X \rightarrow A \rightarrow X \dots$. We performed this counting four times for each T_X with different random number sequences [i.e., four sets of $N (= N_f + N_p) = 10$ samples]. The average of P is shown in Fig. 10 varying T_X from 1.2 to 1.5. P is almost 0 near $T=1.35$. This temperature indicates the marginal point for the switching where large fluctuations of N_f occur. In the range $T \leq 1.25$ or $T \geq 1.45$, motion of the magnetization is very reliable, i.e., $P \approx 1$. In the figure we also plot the square of magnetization per site, $\langle M^2 \rangle / L^3$, during the illumination. The T_X dependence of the magnetization is rather mild while the change of N_p is sharp.

Let us now demonstrate the reversible switching. In order to realize reliable switchings we choose the points, B and C. The dynamics of magnetization is shown in Fig. 11 for the change $[A \rightarrow B \rightarrow A \rightarrow C \rightarrow A \rightarrow B \rightarrow A \rightarrow C \dots]$, where the state at point A is ferromagnetic (α') after coming back from point B and it is paramagnetic (α) after coming back from point C. We regard point B as the state during illumination with the frequency ν_1 and point C as the state during illumina-

tion with the frequency ν_2 . The state at point A is switched by the illuminations of the frequencies ν_1 and ν_2 from α to α' and from α' to α , respectively. In this way the reversible magnetization process is demonstrated. If the temperature at point B becomes lower and the temperature at C becomes higher, the switching becomes more reliable.

As reported in the experiment,^{3,4} light with shorter wavelength was used for switching to the ferromagnetic state. Generally we expect that illumination at short wavelength causes large renormalization of the parameter, although the renormalization depends on the microscopic properties of the individual material. In the above demonstration, we chose a higher temperature to switch off the magnetization. Intuitively this choice is not consistent with the experimental situation. Thus we demonstrate the switching taking another point for C. Here we take the point ($D=3.1, T=1.0$) instead of C. This new point will be called C'. It would be plausible that the renormalized values of D and T shift from A to B through C' with a change of the frequency of the light. The dynamics of magnetization for the change $[A \rightarrow B \rightarrow A \rightarrow C' \rightarrow A \rightarrow B \rightarrow A \rightarrow C' \dots]$ is found to be very similar to that in Fig. 11 and we also find steady reversible switching.

IV. SUMMARY AND DISCUSSION

We have shown that switching of macroscopic states is possible in a sequence of parameter changes of the system, which would model reversible switching in the experiments of photoinduced ferrimagnetism. So far the switching mechanism has been discussed within the picture of the adiabatic potential for the nonmagnetic ground state and magnetic excited state in a microscopic structure. Such micro-

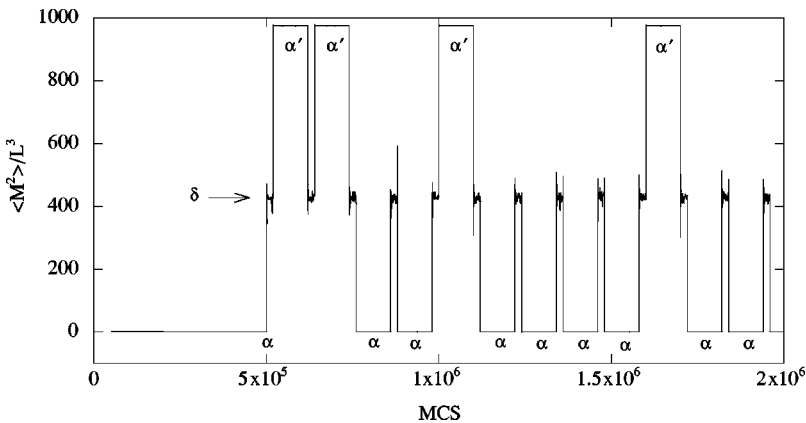


FIG. 9. The change for the square of magnetization per site $\langle M^2 \rangle / L^3$ in the case of $T_X = 1.38$. α and α' denote the paramagnetic state and ferromagnetic state at A, respectively. δ is a state at $T_X = 1.38$.

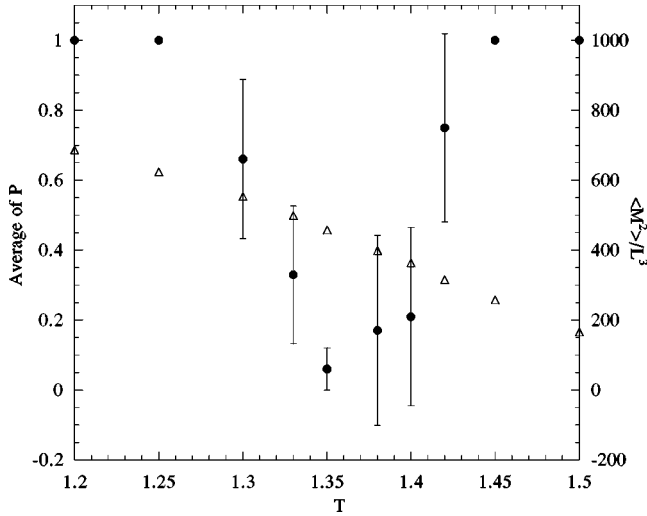


FIG. 10. The closed circles denote average of the reliability P as a function of T_X for fixed $D_X=2.8$. The triangles denote the square of magnetization per site $\langle M^2 \rangle / L^3$.

scopic structure is the necessary condition for the reversible switching. In order to explain the change of macroscopic state, we need to understand how the macroscopic order parameter behaves.

We proposed that the existence of metastability due to the competition between the magnetic coupling and local excitation energy gives an essential mechanism of such a switching. We have investigated thermodynamic properties of the BC model. In particular the metastable ferromagnetic region of the model was studied in detail by a mean-field theory and a Monte Carlo method. The metastable ferromagnetic region was found to be very long-lived. We used this model to explain the reversible switching phenomena. On the assumption that photon's effect causes renormalizations of (D, T) , we observed the dynamics of magnetization for variety of changes of the parameters (D, T) . We demonstrated that in suitable changes of (D, T) the state of the system can be switched to a different one even if the parameters of the system comes back to the original values, which is the essential property of the reversible magnetic switching. The present study thus provides a statistical mechanical mechanism for such switching. We found thermodynamical properties of the switching, such as dependence on the temperature and field, etc., and the reliability of the switching.

In this paper we studied a very simplified model but we

could provide more realistic models which are close to the experimental situation. For example, $\mathcal{H} = -J \sum_{\langle ij \rangle} S_j \sigma_i \tau_j \mu_i + D_\tau \sum_{i \in \Lambda_1} \tau_i^2 + D_\mu \sum_{i \in \Lambda_2} \mu_i^2$ [$J < 0$ (antiferromagnetic), $D_\tau > 0, D_\mu > 0$] would describe the Prussian blue analogs, where $S_i = \pm 3/2, \pm 1/2$ and $\sigma_i = \pm 1/2$. τ and μ take 0 or 1, representing the nonmagnetic or magnetic state. Here Λ_1 and Λ_2 denote the sublattices of the lattice. The $\langle ij \rangle$ denotes all nearest-neighbor pairs. In the future, when more extensive experimental data becomes available, we intend to investigate this kind of detailed model. Furthermore making use of other models with the first-order phase transition, we could provide models for different kinds of switchings, such as a switching between several values of magnetization, etc.

In order to study the phenomena microscopically, we have to know how the parameters (D, T) are renormalized during the illumination. Dependence of the parameters on the frequency and/or the amplitude of light is a challenging problem which we would like to study in the future.

ACKNOWLEDGMENTS

The authors would like to thank Dr. O. Sato for his kind discussion on the experiments and also thank Professor K. M. Slevin for his kind critical reading of the manuscript. The present work was supported by Grant-in-Aid for Science Research on Priority Areas (No. 10149101 ‘‘Metal-assembled complexes’’) from the Ministry of Education, Science and Culture of Japan.

APPENDIX: THE SPONTANEOUS MAGNETIZATION

We determined the boundary in Fig. 4 as the highest temperatures at which the system does not have the magnetization below $M = 0.5L^3$ during the simulation even for $D < D_t$ where the second-order phase transition takes place. In this criterion, if the equilibrium spontaneous magnetization $M_s(T)$ is less than $M = 0.5L^3$, the temperature T belongs to the right-hand side region of the boundary (T is higher than the boundary), although this temperature T is lower than the phase transition point $T_c(D)$. Furthermore, even if the equilibrium magnetization is larger than $M = 0.5L^3$, the system can have the magnetization of $M < 0.5L^3$ as a fluctuation. Thus the boundary in the present criterion locates on the low-temperature side of the true phase boundary.

Generally the spontaneous magnetization M_s changes very rapidly with the temperature and the point at which

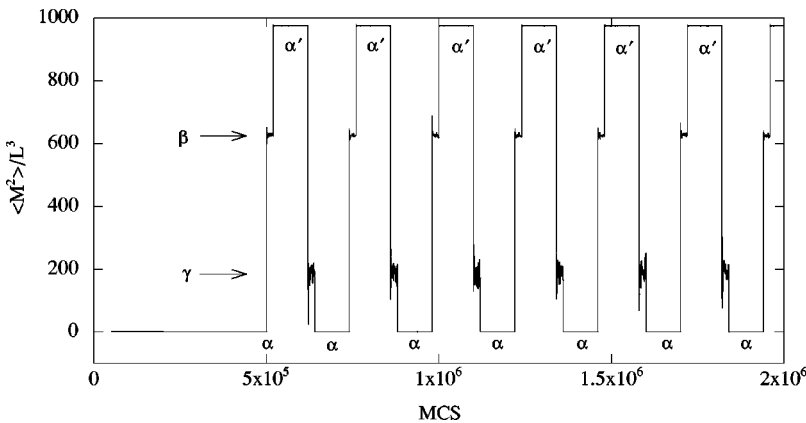


FIG. 11. The change for the square of magnetization per site $\langle M^2 \rangle / L^3$ in the case of choosing $B = (D = 2.8, T = 1.25)$ and $C = (D = 2.8, T = 1.5)$. α and α' denote the paramagnetic state and ferromagnetic state at A, respectively. β and γ are states at B and C, respectively.

$M_s = 0.5L^3$ is very close to the phase-transition point. For the two-dimensional Ising model on the square lattice, the spontaneous magnetization per spin is given by Yang's well-known solution:²² $m_s = [1 - (\sinh 2\beta J)^{-4}]^{1/8}$. Here $k_B T_C / J = 2.2692$ and $k_B T_{1/2} / J = 2.2674$ for $m_s = 0.5$. This temperature for $m_s = 0.5$ is very close to T_C : $T_{1/2} / T_C = 0.999$. The present model is three dimensional and the change of mag-

netization is milder than that of the 2D model because the exponent β is about 0.32 instead of 1/8. However, $m_s(T)$ still shows a very sharp change around T_C as shown in Ref. 23.

Thus the difference discussed above is mainly due to the latter reason, i.e., a fluctuation of the magnetization. In fact the boundary in the system of $L=20$ it is found to locate closer to the phase-transition point.

-
- ¹A. Hauser, J. Adler, and P. Gütlich, Chem. Phys. Lett. **152**, 468 (1988).
- ²P. Gütlich, A. Hauser, and H. Spiering, Angew. Chem. Int. Ed. Engl. **33**, 2024 (1994).
- ³O. Sato, T. Iyoda, A. Fujishima, and K. Hashimoto, Science **272**, 704 (1996).
- ⁴O. Sato, Y. Einaga, T. Iyoda, A. Fujishima, and K. Hashimoto, J. Electrochem. Soc. **144**, L11 (1997).
- ⁵M. Blume, Phys. Rev. **141**, 517 (1966).
- ⁶H. W. Capel, Physica (Amsterdam) **32**, 966 (1966); **33**, 295 (1967); **37**, 423 (1967).
- ⁷M. Blume, V. J. Emery, and R. B. Griffiths, Phys. Rev. A **4**, 1071 (1971).
- ⁸G. D. Mahan and S. M. Girvin, Phys. Rev. B **17**, 4411 (1978).
- ⁹A. Benyoussef, N. Boccara, and M. El Bouziani, Phys. Rev. B **34**, 7775 (1986).
- ¹⁰N. S. Branco and B. M. Boechat, Phys. Rev. B **56**, 11 673 (1997).
- ¹¹M. Tanaka and T. Kawabe, J. Phys. Soc. Jpn. **52**, 2194 (1985).
- ¹²Y. Aoyama, W. Chen, and M. Tanaka, J. Phys. Soc. Jpn. **66**, 272 (1997).
- ¹³D. M. Saul, M. Wortis, and D. Stauffer, Phys. Rev. B **9**, 4964 (1974).
- ¹⁴A. K. Jain and D. P. Landau, Phys. Rev. B **22**, 445 (1980).
- ¹⁵D. P. Landau and R. H. Swendsen, Phys. Rev. Lett. **46**, 1437 (1981).
- ¹⁶M. Deserno, Phys. Rev. E **56**, 5204 (1997).
- ¹⁷T. Fiig, B. M. Gorman, P. A. Rikvold, and M. A. Novotny, Phys. Rev. E **50**, 1930 (1994).
- ¹⁸E. N. M. Cirillo and E. Olivieri, J. Stat. Phys. **83**, 473 (1996).
- ¹⁹K. Binder, Z. Phys. B **43**, 119 (1981).
- ²⁰J. Lee and J. M. Kosterlitz, Phys. Rev. Lett. **65**, 137 (1990).
- ²¹P. A. Rikvold, H. Tomita, S. Miyashita, and S. W. Sides, Phys. Rev. E **49**, 5080 (1994).
- ²²C. N. Yang, Phys. Rev. **85**, 808 (1952).
- ²³N. Ito and M. Suzuki, J. Phys. Soc. Jpn. **60**, 1978 (1991).